ISSN:1687-1006

The Egyptian International Journal of Engineering Sciences and Technology

Vol. 30 (2020) 79–89

https://eijest.journals.ekb.eg/

Repairing Capability of Friction Stir Welded Defected SAF 2205 Duplex Stainless Steels Groove Joints Using Fusion Welding Processes

K. A. Abdelazem[a*] , H.M. Abd El-Aziz [b] , M.M.Z. Ahmed[c] , I.G. El-Batanony[d]

[a] *PhD student, PETROJET Company, Joseph teto St., Hayekstep, Cairo, Egypt*

[b] *Asst. Prof., Mining and petroleum Dept., Faculty of Engineering, Al-Azhar University, Alnasr St., Cairo, Egypt*

[c] *Prof., Metallurgical and Materials Engineering Department, Faculty of Petroleum and Mining Engineering, Suez University, 43721, Salah Nessim St., Suez, Egypt*

[d] *Prof., Mechanical Engineering Dept., Faculty of Engineering, Al-Azhar University, Alnasr St., Cairo, Egypt*

ARTICLE INFO

Keywords:

1st Duplex stainless steel
2nd repair
3rd Friction stir welding
4th Groove joint
5th fusion welding

ABSTRACT

This work focuses on studying the repairing capability of defected 6.5 mm-thick SAF 2205 duplex stainless steel (DSS) plates, welded using friction stir welding and repaired using fusion welding processes, shielded metal arc welding (SMAW), and gas tungsten arc welding (GTAW). A special tool made of tungsten carbide (WC) based material, with dimensions of 12 mm pin diameter, 5.5 mm pin length, and 20 mm shoulder diameter was used, the friction stir welding (FSW) parameters were, rotational speed of 300 RPM, travers speed of 25 mm/sec, and the tool was tilted 3˚. Variant designs of V grooved joint geometries, with different groove angles, and 2mm root face, were used without root opening. The welded joints were inspected using both visual test (VT) and radiographic teste (RT). The mechanical properties, corrosion resistance, micrograph, microstructure, and the balance between ferrite and austenite phases, were investigated and analyzed for the repaired joints. It was significantly observed that, the repaired joints were sound with good quality, good mechanical properties, good interface between weld metal and base metal, good balance between ferrite and austenite phases, and their corrosion resistance is better than base metal.

1. Introduction

The UNS designation for SAF 2205 is S31803/S32205, SAF derives from Sandvik Austenite Ferrite [Material data sheet for SAF 2205 issued by Sandvik]. DSS finds an increasing application in the chemical, oil and gas industries, petrochemical processing plants, pulp and paper industry, pollution control equipment, transportation and general engineering thanks, due to its high corrosion resistance and mechanical properties [1]. High corrosion resistance and a good combination with mechanical properties of DSS can be explained by chemical composition and balanced "dual" microscopic structure for roughly equivalent fractions of ferrite and austenite. First, the chemical composition based on the high content of Cr and Mo improve the pitting and intergranular corrosion resistance, respectively. Moreover, nitrogen additives can promote structural solidification through a solid interstitial solution mechanism, which increases the yield strength and final strength values without damaging the rigidity. Second, the two-stage microstructure ensures higher resistance to cracking and corrosion caused by traditional stainless steel [2].

This type of stainless steel has the advantages of both ferrite and austenitic stainless steels individually.

The mechanical properties and the corrosion

* Corresponding author. Tel.: +2010-060-48873.
E-mail address: kabdelazem@yahoo.com

resistance of austenitic stainless steels are improved with the presence of ferrite phase [3-4]. In this metal, nobler properties are achieved when the material has equal proportions of austenite and ferrite, in general, the range of ferrite level at DSS weld metals is 30-70% according to the composition and the rate of cooling [5].

DSS fusion welding produces a microstructure consisting of coarse ferrite granules, and both intergranular and intragranular austenite phases inside the welding metal and heat affected zone (HAZ). The preferred dual microscopic structure of this stainless steel is destroyed by applying the traditional fusion welding processes. It was shown that SAF 2507 DSS ferrite content ranging between 50 and 60% across weldments produced by FSW, which is slightly higher than the based material [6].

It was found that, the austenite formed is higher in root zone than that of weld cap. There are coarse ferrite grains observed in weld cap zone. When the welding was carried out with higher heat input (i.e. slower cooling rate), large grain size and higher contents of austenite were noted for DSS and SDSS welds. With lower heat input (i.e. higher cooling rate), lower finer grains austenite content was observed for DSS and SDSS welds. In HAZ, an increase in grain size was observed due to re-crystallization, especially in ferrite, there was a formation of inter-granular and intra-granular austenite in this zone. It was noted that the weld cap contains more ferrite than the root region for the both fusion zone and the heat affected zone. It can also be noted that ferrite volume fraction in HAZ is higher than that of the weld region [7].

The required phase ratio changed during fusion welding processes and encourages the formation of more ferrite in the weld metal as a result of the re-melting and solidification of the material [4-9].

Mourad et al. [10], stated that for tensile test of 2205 DSS specimens welded using the GTAW process and ER 2205 filler showed that, the ductile fracture occurred at HAZ and base metal, and the results were 450 MPa, 621MPa, and 25% for Yield strength, Ultimate strength, and elongation percentage respectively

Aristotile et al. [11], stated that, Anyway, even in the most critical conditions, higher impact values are required for service temperatures around -40 to -50 °C. About 70 to 75 Joules are the values obtained in this temperature range, which guarantee good service performance at these temperatures

Vise verse, solid-state welding techniques such as FSW appear to be an appropriate technique in this respect [8]. This process reduces the problem of ferritization in DSSs during welding thermal cycles due to their solid state nature, and minimizing the fusion welding problems [8,12].

There is a lot of interest in FSW for DSS. An important feature of FSW is that, it greatly refines ferrite (α) and austenite (γ) granules without altering the appropriate phase balance in the DSS, and thus, increases the hardness and strength of the stirring zone (SZ) [6,13]. Electron backscattering diffraction (EBSD) analysis of the microstructure in the friction stir welds of SAF 2507 revealed the development of grain refining by dynamic recrystallization in both component phases [2].

After FSW of DSS, grain sizes of both ferrite and austenite were reduced in the stirring region, resulting in higher hardness and strength [5]. In addition, the increase in welding speed reduces the peak temperature and the duration of high temperature in the stirring region, thereby reducing the α and the γ granule size and increasing the hardness of the stirring region [13-15]. Another benefit of high welding speed is that when the peak temperature is less than the transition temperature α to γ, the desired ratio of α/γ can be achieved in the weldments. Moreover, FSW can be used to improve the cavitation erosion resistance of DSS [16].

It is noted that, defect free welds with good appearance with improving mechanical and corrosion resistance properties were obtained for V joints with, 60˚ groove angle, 2 mm root face, no root gap and welded using FSW process, with fixed welding parameters, as traverse speed of 25 mm/min, rotating speed of 300 rpm, axial load of 20 KN, and 3˚ tilt angle, Vise verse, defected joints was produced when using V joints with 40 groove angle, and V joints with 60 groove angle, and 1 mm raised face [17].

The objective of the present work is to study the repairing capability of friction stir welded defected SAF 2205 DSS Groove Joints, using fusion welding, SMAW and GTAW processes.

2. EXPERIMENTAL WORK

2.1 Material

The material used are SAF 2205 duplex stainless steel plate of 6.5 mm thickness, with chemical composition and mechanical properties as shown in Tables 1-2, FSW tool made of tungsten carbide (WC) based material, and filler wires ER2209 and E2209.

Table 1. Chemical composition of the SAF 2205 duplex stainless steel plates base metal (in wt. %).

Componen	C	Si	Mn	P	S	Cr	Ni	Mo	N
Reference[1]	0.03	1.0	2.0	0.03(	0.02(	22-2	4.5-6.	3-3.5	0.14-0.
Base metal	0.015	0.38	1.51	0.025	0.001	22.43	5.74	3.15	0.17

[1], single values are the maximum.

2.2 Friction Stir Welding

The FSW welding was carried out using the FSW machine model (EG-FSW-M1) shown in Fig. 1, at the friction stir welding and processing lab that belongs to Faculty of Petroleum and Mining Engineering, Suez University. The tool was controlled vertically, but the work peace was controlled horizontally. WC tool specially designed for this work, the probe of conical shape,12/5 mm diameters, with a length of 5.5 mm, and a shoulder of 20 mm diameter shown in Fig. 2. The FSW applied with constant rotational speed at 300 rpm, travel speed at 25mm/min, tilt angle of 3°, and down load of 20KN [17]. The joints were prepared as V grooved geometry without root opening, and 2 mm root face, for both joints and 40° groove angle for specimen 1 and 60° with 1 mm raised face at shoulder land for specimen 2 shown in Fig. 3

Fig. 1, Friction Stir Welding Machine

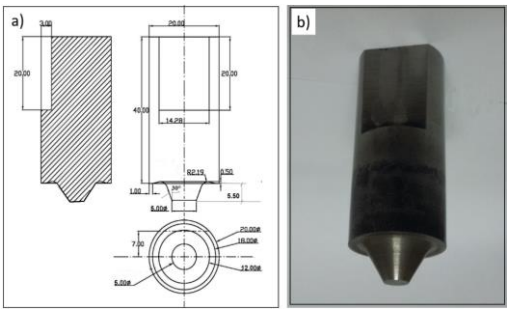

Fig. 2, (a) Design drawing of tungsten carbide tool, (b) An image of the tungsten carbide tool used

2.3 Fusion Welding

After determining the defected joints, it will be prepared, and the defects will be removed using the grinding machine. Specimens were repaired by applying the traditional fusion welding processes, SMAW for joint specimen 1 and GTAW for joint Specimen 2. SMAW process was applies using direct current electrode positive (DCEP) and welding parameters of, 27-29 V volt, 80-85 A current, 900 - 1133 J/mm Heat Input, using E2209 as a filler wire. GTAW process was applied using direct current electrode negative (DCEN) and welding parameters of tungsten electrode 2.4 mm type EWTH-2 (2% Thoriated), 10-15 L/min argon flow rate, 10-14.5 V volt, 116 -159 A current, 766 - 1548 J/mm heat input, using ER2209 as a filler wire. Prior to welding, the joints were mechanically cleaned using stainless steel wire brush to remove surface oxides and contaminations. For convenience and ease in identifying specimens, the designations Sp1R, and Sp2R were selected for repairs specimens 1 and 2 respectively.

Table 2. mechanical properties of SAF 2205 duplex stainless steel plates base metal

Component	Tensile strength (MPa)	Yield strength (MPa)	Elongation %	Hardness	
				Brinell	Rockwell
Reference	655	450	25	293	31
Base metal	822	700	33	245	26

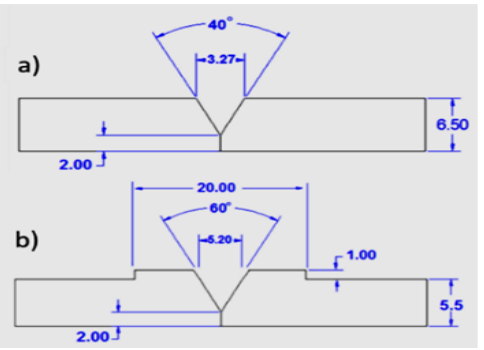

Fig. 3, V groove design, with 2 mm root face, and no root gap for, a) Specimen 1, 40° groove angle, and b) Specimen 2, 60° groove angle, 1 mm raised face

2.4 Nondestructive Tests (NDT)

Visual test (VT) and radiographic test (RT) should be applied on the welded and repaired joints to determine the defected areas, and to make shore that, the repaired joints are sound and free from defects, before preparing them for microstructure

investigation, and mechanical test evaluation, VT was applied on welded beads using naked eyes and welding gage, RT had been carried out on welded beads using Gama ray camera with Iridium-192 radiation source, D7 radiographic films, and applying single wall single image technique.

2.5 Destructive Test (DT)

The sound repaired joints, had been cut out into test samples for DT such as tensile, bending, and impact to ensure the suitability of the repaired joints, to withstand the applied stresses, and corroded service, shown in Fig. 4.

2.5.1 Tensile Test

Tensile test was conducted using the universal testing machine (Tinius Olsen) shown in Fig. 5, which located at PETROJET central workshop - Cairo, 600 KN capacity with a speed of 0.05 mm/Sec, according to ASME IX and ASTM E8 [18,19]. To evaluate the tensile properties of the repaired joints, large transverse flat tensile specimens with a gauge length of 50 mm and a width of 12.5 mm were machined perpendicular to the welding direction. Tensile tests were carried out at room temperature, the failure load and failure location were recorded for each specimen, where the failure load was the averaged of two specimens for each welding condition shown in Fig. 4a.

2.5.2 Bend Test

Three-point bend tests were applied using a universal testing machine (Tinius Olsen) shown in Fig. 5, which located at PETROJET central workshop – Cairo, with a crosshead speed of 0.5 mm/min according to ASME IX [18]. The cap and root-bead reinforcements were removed flush with the surfaces to be smooth, the specimen dimensions were 200 x19 x 6.5 mm as shown in Fig. 4b, the test was carried out at room temperature, the test load was 59 KN, the specimens were bent in a U-shaped, the weld root surface becomes the convex surface, and visually examined for cracks or any other imperfection.

2.5.3 Impact Test

Impact test was carried out using a specially designed testing machine (Tinius Olsen) Model IT 542, it has an available energy of 542 J, and located at the PETROJET central workshop laboratory, Cairo shown in Fig. 6, according to ASME IIIV, and ASTM E-23 [20-21] at -40°C. Three specimens of 50 x 10 x 6.5 mm thickness. The notch was made at both weld metal centerline, and weld line intersection with HAZ at mid-thickness of the specimens, the average of three specimens for each set will be the energy absorbed.

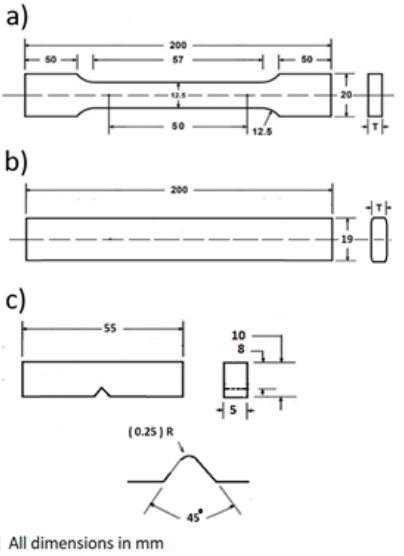

Fig. 4. Test samples plot of welded specimen for, a) Tension test , b) Bend test, c) Impact test

2.6 Macrograph and Microstructure

The joints were evaluated using both macrograph to reveal the appearance of the joint cross section, and microstructure analysis to reveal the internal structure, grain size, and grain distribution of the joints due to welding processes. Transverse to the weld centerline sections were taken in order to include full weld cross section containing fusion zone (FZ), stir zone (SZ), thermo-mechanically affected zone (TMAZ), heat affected zone (HAZ), and base metal (BM). Each specimen was prepared properly through basic steps according to ASTM E-3 [22] and ASTM E-2014 [23], the welded specimens were polished up to 1200 grit fineness, which was followed by a cloth polishing with 0.5 μm alumina paste, cleaning with acetone and then dried, later, the specimens were electrochemically etched by 20 g KOH, and100 ml H2O solution, to reveal the microstructure, using 6V DC source, for 15 sec. Microstructure will applied using optical microscopy, located at Egyptian British University (BUE), Cairo.

Fig. 5. Tensile / Bend test machine

Fig. 6. Impact test machine

2.7 Ferrite Number Measurements

According to ASTM E562 [24], and using of the ferrite-scope (Fischer FERITSCOPE MP30), the ferrite levels were measured and reported as ferrite number "FN" a proper measurement surface are used, where the cross section of the welds shall be ground flat as a minimum 400 grit wheel finishing grinding and free from any foreign material. The ferrite readings can be obtained with the probe in use. A corrective calibration of the equipment shall be performed whenever the probe is changed.

2.8 Corrosion Behavior Testing

The technique of Potentiodynamic testing was applied to study the corrosion behaviour of the weldments, according to ASTM G5[25] and ASTM G3 [26], the test was carried out at 22±1 °C, in 3% wt NaCl aqueous solutions, the specimen's dimensions were 6.5 x 20 x 10 mm, the preparation of the specimens according to ASTM E3 [22], The corrosion resistance rate will be measured in millimetre per year (mmpy).

3. RESULTS AND DISCUSSION

The results of non-destructive test, destructive test, macrograph evaluations, microstructure investigations, and ferrite number measurement, will be discussed and analyzed in order to evaluate and characterize the repaired joints.

3.1 Non-destructive Tests (NDT) Results

Visual and radiographic testing for joint specimen 1, with 40° V grooved angle, and 2 mm root face as a joint design, beside its bad appearance, it is observed that; A cavity at advancing side, almost along the joint length, Fig. 7. For joint specimen 2, where a special design, with 60° V grooved angle with 2 mm root face, and 1 mm raised face at shoulder land, as a joint design. It is noted that although this joint has no reduction in thickness and good appearance; Nevers less an internal cavity observed almost along the joint length at advancing side, due to lack of material flow shown in Fig. 8. Moreover, specimens1 and 2, Repaired (Sp1R) and (Sp2R), which repaired by traditional fusion welding processes, SMAW and GTAW, respectively, there is a good appearance for both two joints. In addition, Radiographic film's interpretation shows sound free from defects welds for both, shown in Figs. 9 and 10.

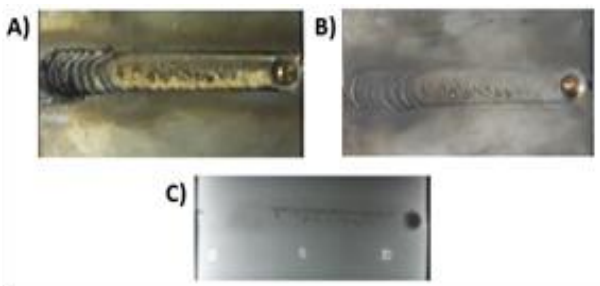

Fig.7, Specimen 1, welded by FSW process, a) Visual appearance with flash, b) Visual appearance without flash, c) Radiography.

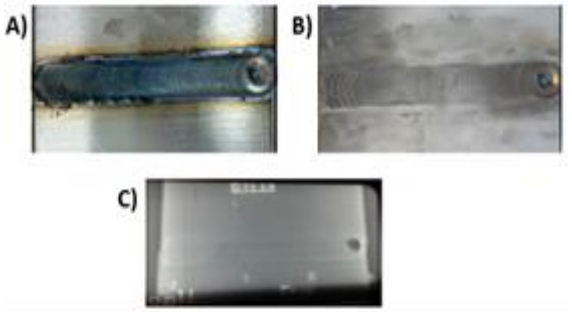

Fig. 8, Specimen 2, welded by FSW process, a) Visual appearance with flash, b) Visual appearance without flash, c) Radiography

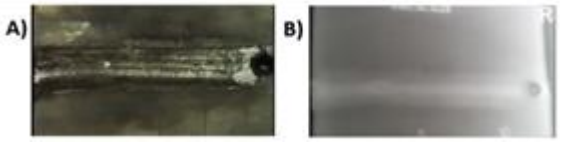

Fig. 9, Sp1R, after repair, a) visual appearance, b) Radiography

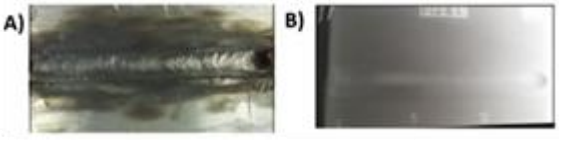

Fig. 10, Sp2R, after repair, a) Visual appearance, b) Radiography

3.2 Destructive Test Results

3.2.1 Tensile Test Results

For joint Sp1R, which repaired using SMAW, the average values were; yield stress 565 MPa, ultimate tensile stress 765 MPa, and 40% elongation, which are more than the minimum requirements of base metal, and the fracture occurred at base metal. For joint Sp2R, which repaired by GTAW, the average values were; yield stress 590 MPa, ultimate tensile stress 768 MPa, and 38% elongation, which are more than the minimum requirements of base metal, shown in Fig. 11, with ductile fracture appearance for both two joints, these results better than that obtained by Mourad et al [10]. In addition, stress, strain and young's modulus can be calculated for specimens 1R and 2R, as shown below;

$\sigma_y = F_y / A$, $\varepsilon_y = \sigma_y / E$, $E = \sigma_y / \varepsilon_y$
$\sigma_u = F_u / A$, and $\varepsilon_u = \sigma_u / E$ where;
σ_y; yield stress, F_y; yield force, A; cross sectional area, ε_y; yield strain
σ_u; ultimate tensile stress, F_u; ultimate force, ε_u; ultimate strain, E; young's modulus

The test data for specimens 1R and 2R from Fig.11 as shown in Table 3

Table 3, Tensile test data for specimens 1R and 2R

Specimen	Area (mm2)	F_y (KN)	F_u (KN)	Offset
1R	79.55	44.9	60.85	0.27%
2R	73.15	43.1	56.2	0.26%

For specimen 1R
$E = \sigma_y / \varepsilon_y$
$\sigma_y = F_y / A = 44.9/ 79.55 = 0.565$ KN/mm2
$= 565$ MPa
$\varepsilon_y = 0.0027$ at 0.27% offset
$E = 565 / 0.0027 = 209.259$ GPa
$\sigma_u = F_u / A = 60.85/79.55 = 0.765$ KN/mm2
$= 765$ MPa
$\varepsilon_u = \sigma_u / E = 765/209259 = 0.00365$

For specimen 2R
$E = \sigma_y / \varepsilon_y$
$\sigma_y = F_y / A = 43.1/ 73.15 = 0.590$ KN/mm2
$= 590$ MPa
$\varepsilon_y = 0.0026$ at 0.26% offset
$E = 590 / 0.0026 = 226.923$ GPa
$\sigma_u = F_u / A = 56.2/73.15 = 0.768$ KN/mm2
$= 768$ MPa
$\varepsilon_u = \sigma_u / E = 768/226923 = 0.00338$

3.2.2 Bend Test Results

For bent specimens of repairing joints, Sp1R and Sp2R it was observed that, no cracks were observed as shown in Fig. 12, this could be related to the information of sound welds, according to ASME IX [18], so bend test was considered acceptable.

3.2.3 *Impact Test Results*

The impact energies of weld metal centerline and HAZ, as shown in Fig. 13, show that, the average toughness at -40°C, for weld metal and HAZ of Sp1R which, repaired by SMAW, were 80 and 85 J respectively, these results are accepted according to ASTM A923 [27], and agree with the results of Aristotile et al [11]. On the other hand, for joint Sp2R which, repaired by GTAW, were 27, 70 J respectively, these results are accepted for HAZ, not accepted for weld metal according to ASTM A923 [27], and not agree with the results of Aristotile et al [11]. Moreover, it was noted that, for joint Sp1R not only strength was improved but the toughness was improved as well, for joint Sp2R the strength was

improved but the toughness was not improved.

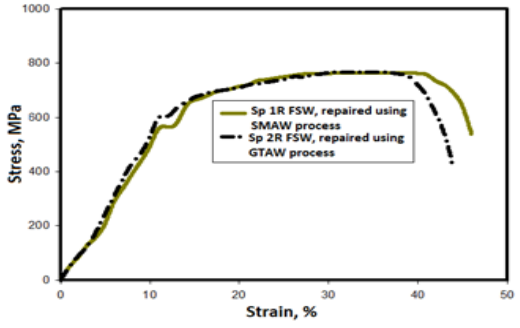

Fig. 11, Stress strain diagrams, for Specimen 1R repaired by SMAW, and Specimen 2R repaired by GTAW

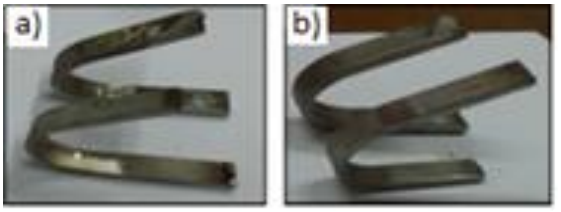

Fig. 12, Bent specimens of FSW welded joint, and repaired by a) SMAW joint Sp1R, b) GTAW joint Sp2R

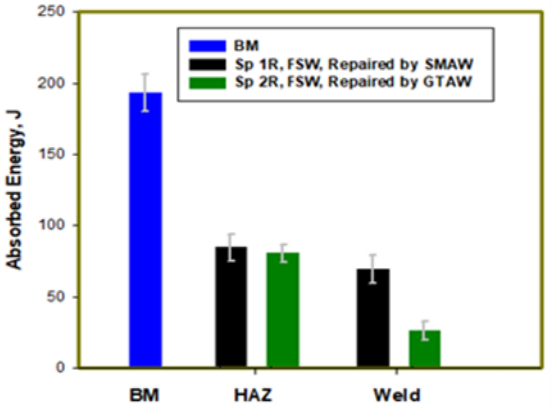

Fig. 13, Bar chart with error bars for Impact test at - 40°C of BM, joint Sp1R repaired by SMAW, and joint Sp2R repaired by GTAW.

3.3 Macrograph and Microstructure Results

The macrographs of the transverse cross-sections of joints Specimens 1R and 2R, which welded by FSW and repaired by traditional fusion welding SMAW and GTAW respectively, as shown in Figs. 14A, and 15A, it was noticed that, there is a defect free cross section with good interface between original welds which welded by FSW process, and the repaired welds which welded by fusion welding processes.

The microstructure of joint No. Sp1R which, repaired by SMAW shown in Fig.14, area B represents the as received base metal with the wrought DSS typical microstructure, it is observed that, the ferrite content was about 49%, and the austenite content was about 51%, area C represents HAZ for FSW, which appears with finer grains, and good distribution between austenite and ferrite phases, area D represents the weld cap region at fusion zone, it consists of grain boundary austenite, intra-granular, and Widmanstten austenite formed in a ferrite matrix [7]. in addition, the coarse ferrite grains were observed, where, the weld cap contains more ferrite, and the austenite grains are slightly smaller than that are in area E, filling region. At area F, there is good interface between fusion zone and stir zone, good distribution between ferrite and austenite phases, and almost no grain gross. In addition, it is noted that, at area G, root region, there is no change in grain size and grain distribution, and both austenite and ferrite, are with fine grains, which resulted from friction stir welding process, this area not affected by reheating and thermal cycles from multi-passes during repairing. Moreover, area H shows the interface between SZ and FZ, HAZ region, there is a slightly ferrite grain gross and almost good distribution between ferrite and austenite phases, and area I shows two HAZs, HAZ 1 represents the interface between FZ and SZ, where, there is a slightly ferrite grain gross and almost good distribution between ferrite and austenite phases, the second heat affected zone (HAZ 2) represents the interface between BM and SZ, where the grains were refined, with good distribution, it is observed that the interface in HAZ 2 is better than that in HAZ 1, and both of them are acceptable. Accordingly, this advantage encourages and support repairing FSW defected joints using traditional fusion welding SMAW process.

For joint Sp2R which, welded by friction stir welding, and repaired by GTAW shown in Fig. 15, it is noted that, area B represents the as received base metal, area C represents HAZ for FSW, which appears with finer grains than the as received base metal, area D represents HAZ for fusion zone which contains ferrite and austenite coarse grains. At area E, which represent cap zone, there is a heterogeneous distribution between ferrite and austenite grains. Area F, which represent the interface between stir zone and fusion zone, it is noted that, there is a bad interface between the fusion zone and the stir zone, bad distribution between ferrite and austenite phases, and almost austenite free area with ferrite coarse grains

At area G which represent the root zone there is a microstructure consisting of coarse ferrite grains and irregular distribution of the austenite grains inside the ferrite matrix. In addition, it is noted that, there is a higher amount of austenite formed at root, than both of filling and weld cap, this amount of austenite, was formed due to the weld root region was subjected to reheating due to multi passes during welding, which resulted in lower cooling rate than both filling and cap at F and E regions, respectively [7,15].

Both of regions H and I are representing the interface between FZ and BM at the friction stirred areas, where there are almost austenite free areas with ferrite coarse grains.

From macrographs and microstructures shown in Figs. 14 and 15, it is extremely noted that, there are a fairly good interface between FZ and SZ, and finer grains with almost homogeneous distribution of both austenite and ferrite grains for joint Sp1R which, repaired using SMAW process, than that of joint Sp2R, which repaired using GTAW process. Thereby, SMAW process, is a completely nobler in repairing SAF 2205 DSS FSW defected groove joints than GTAW process.

3.4 Ferrite Content Measurement Results

Ferrite content profiles for the joints Sp1R, and Sp2R, show that, the average ferrite/austenite content for joint Sp1R at weld metal and HAZ were 39/61, and 41/59 respectively shown in Fig.16A, and for joint Sp2R at weld metal and HAZ were 43/57, and 48/52 respectively shown in Fig. 16B. From Fig. 16C, It can also be noted that ferrite volume fraction at HAZ is higher than that of the weld region and that is agree with Paulraj et al [7]. It is significantly noted that, FN for Sp2R is higher than FN for Sp1R, and that is confirm the microstructure evaluations across HAZ and FZ of these joints shown in Figs. 14 and 15, it is attributed to exposing the joint welded using GTAW process to lower heat input and higher cooling rate during weld than that of the joint welded by SMAW process, where, the ferrite is more than the austenite at the higher temperatures in DSS, and the time to reformation of austenite in is less than that for joints welded by SMAW process [7,15]. In general, it is observed that, the ferrite level at DSS weld metal is within the range of 30-70% and agree with Robert et al [5].

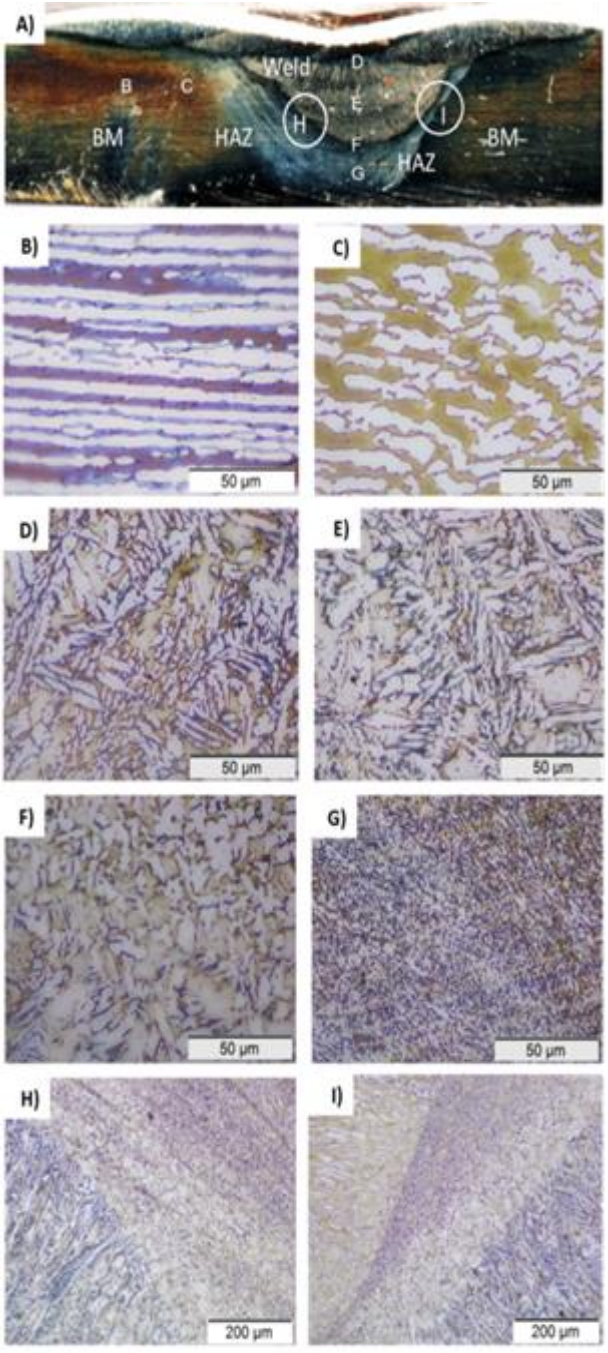

Fig.14, Specimen 1R, welded by FSW process, and repaired by SMAW process, A) Macrograph, and B), C), D), E), F), G) Microstructure with magnification of 50X, H), and I) Interface microstructures with magnification of 10X

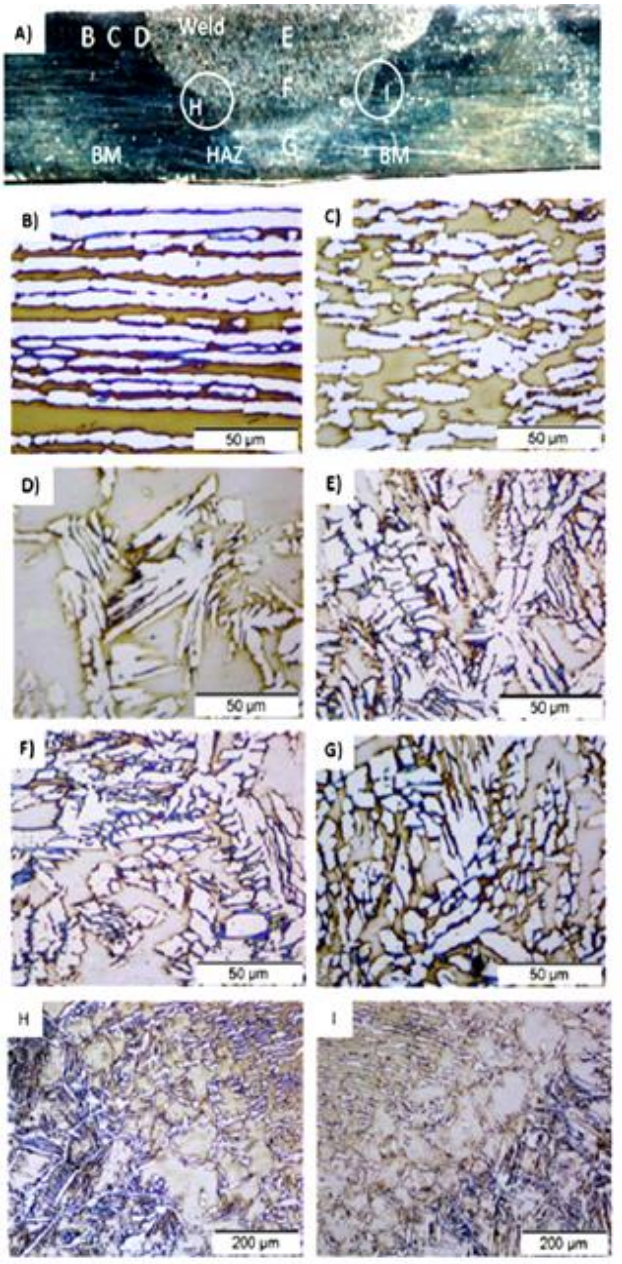

Fig.15, Specimen 2R, welded by FSW process, and repaired by GTAW process, A) Macrograph, B), C), D), E), F), G) microstructure with magnification of 50X, H), and I) Interface microstructures with magnification of 10X

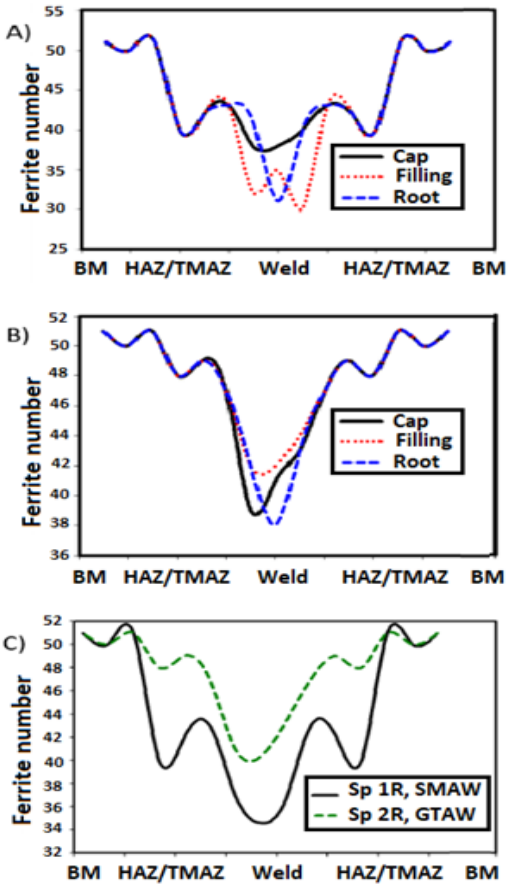

Fig. 16, Ferrite number diagram for, a) Sp1R joint, b) Sp2R joint, c) Comparison between joints Sp1R, and Sp2R.

3.5 Corrosion Test Results

The average corrosion rates of SAF 2205 DSS base metal, joint Sp1R and joint Sp2R were 3.4522, 0.02098, 0.59187 mmpy respectively, these results are accepted according to ASTM A923 [27]. In addition, it was noted that the corrosion resistance for SP1R is better than Sp2R and the both as a whole nobler than BM shown in Fig. 17, that is due to the formation of almost austenite free areas with ferrite coarse grains, which resulted in a lower cooling rate of the joints welded using GTAW [7,15]. The required phase ratio changed during fusion welding processes and encourages the formation of more ferrite in the welding metal as a result of the re-melting and solidification of the material, so that is agree with Robert et al [5].

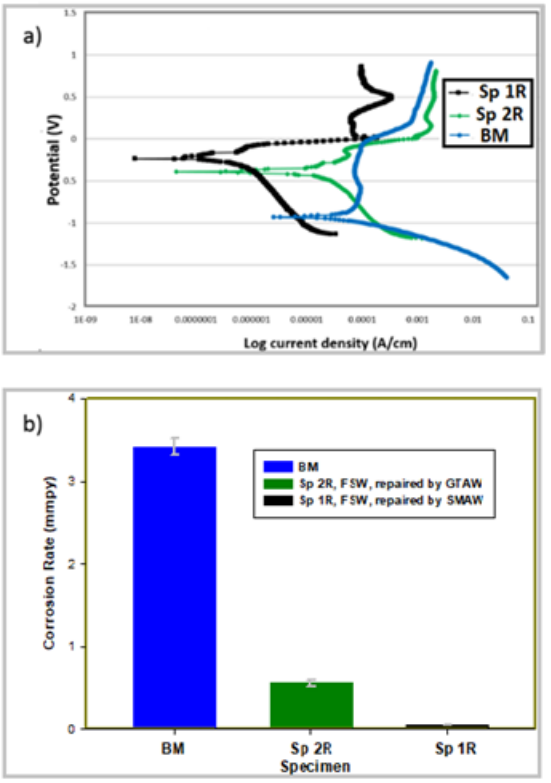

Fig. 17, a) Comparison between Tafel (potentiodynamic) polarization curves for DSS specimens of DSS SAF 2205 BM, joint Sp1R, and joint Sp2R, b) Bar chart with error bars for the average corrosion rates of same specimens

4. Conclusion

The defected groove joints of 6.5 mm thick SAF 2205 DSS plates, which welded using FSW, and repaired using traditional fusion welding SMAW and GTAW were investigated, and it was found that:

1-Sound repaired joints with high continuity appearance were successfully obtained.

2-The repaired joints have good mechanical properties and corrosion resistance.

3- There is an extremely good interface between FZ and both BM and SZ, nevertheless, the interface between FZ and SZ is better than that between FZ and BM.

4- Good balance between ferrite and austenite phases was obtained.

5- SMAW process, is nobler than GTAW process for repairing of 6.5 mm thickness SAF 2205 DSS FSW defected groove joints.

REFERENCES

[1] S. Azuma, K. Ogawa; "Duplex stainless steel excellent in corrosion resistance", Applied Thermal Engineering" Vol. 18, 1998.

[2] I. Álvarez Armas, S. Degallaix Moreuil; "Duplex Stainless Steel", 2009.

[3] P. Sathiya, S. Aravindan, R. Soundararajan, A.N. Haq; "Effect of shielding gases on mechanical and metallurgical properties of duplex stainless-steel welds", Journal of Materials Science, Vol. 44, Pp. 114–121, 2009.

[4] A. Urena, E. Otero, M.V. Utrilla, C.J. Munez; "Weldability of a 2205 duplex stainless steel using plasma arc welding", Journal of Materials Processing Technology, Vol. 182, Pp. 624–631, 2007.

[5] Robert N. Gunn; "Duplex Stainless Steels, Microstructure, Properties and Appls." Abington Publishing, 2003.

[6] Sato Y. S., Nelson T. W., Sterling C. J. Steel R. J., Pettersson C. O.; "Microstructure and mechanical properties of friction stir welded SAF2507 super duplex stainless steel", Mater. Sci. Eng. A, Vol. 397, Pp. 376–384, 2005.

[7] Prabhu Paulraj, Rajnish Garg studie; "Effect of welding parameters on pitting behavior of GTAWof DSS and super DSS weldments", Engineering Science and Technology, an International Journal, Vol. 19, Pp. 1076–1083, 2016.

[8] T. Saeid, A. Abdollah-Zadeh, T. Shibayanagi, K. Ikeuchi, H. Assadi;" On the formation of grain structure during friction stir welding of duplex stainless steel", Materials Science and Engineering, Vol. 527, Pp. 6484–6488, 2010.

[9] B. I. Voronenko, Austenitic; "ferritic stainless a state-of-the-art review", Metal Science and heat Treatment, Vol. 39, pp. 20- 29, 1997.

[10] Mourad A-HI, Khourshid A, Sharef T. Gas tungsten arc and laser beam welding processes effects on duplex stainless steel 2205 properties. Mater Sci Eng A 2012;549:105–13.

[11] Rome R Aristotile, M Barteri & M Fersini:' Weldability of duplex stainless steel using tungsten inert gas (TIG) and submerged- arc welding' Welding International 1993 7 (5) 351-357.

[12] H. Fujii, L. Cui, N. Tsuji, M. Maeda, K. Nakata, K. Nogi; "Friction stir welding of carbon steels", Materials Science and Engineering, Vol. A 429, Pp.50–57, 2006.

[13] T. Saeid, A. Abdollah-zadeh, H. Assadi, F. Malek Ghaini; "Materials Science and Engineering", Vol. A 496, Pp. 262–268, 2008.

[14] Y. Morisada, H. Fujii, R. Nishimoto, T. Miyazawa, Y. Iwamoto, R. Ueji; "Improvement of toughness and strength of thick structural steel weld by friction stir welding" Science and Tech. of Welding and Joining, Vol. 18, Pp. 287–292, 2013.

[15] M. Esmailzadeh, M. Shamanian, A. Kermanpur, T. Saeid; "Microstructure and mechanical properties of friction stir welded lean duplex stainless steel", Materials Science & Engineering, Vol. 561, Pp. 486–491, 2013.

[16] J.D. Escobar, E. Vela´ Velasquez, T.F.A. Santos, A.J. Ramirez, D. Lopez," Improvement of cavitation erosion resistance of a duplex stainless steel through friction stir processing (FSP)", Wear Journal, Vol. 297, Pp. 998–1005, 2013.

[17] Khaled A. Abdelazem, H. M. Abd El-Aziz, M. M. Z. Ahmed, I. G. El-Batanony; "Characterization of Mechanical Properties and Corrosion Resistance of SAF 2205 Duplex tainless Steel Groove Joints Welded using Friction Stir Welding Process", International Journal of Recent Technology and Engineering (IJRTE), Vol.-8 Issue. 6, Pp 3428–3435 March 2020.

[18] ASME, Boiler & Pressure Vessel Code, Section IX;" Qualification Standard for Welding, Brazing, and Fusing

Procedures; Welders, Brazers; and Welding, Brazing, and Fusing Operators", 2017.
[19] ASTM E-8;" Standard test methods for tension testing of metallic materials", 1999.
[20] ASME, Boiler and Pressure Vessel Code, Sec. IIIV Div. 1; "Rules for Construction of Pressure Vessels", 2017.
[21] ASTM E-23; "Standard methods for notched bar impact testing of metallic materials", 2006.
[22] ASTM E-3; "Standard Guide for Preparation of Metallographic Specimens", 2011.
[23] ASTM E-2014; "Standard Guide on Metallographic Laboratory Safety", 1999.
[24] ASTM E 562; "Standard Test Method for Determining Volume Fraction by Systematic Manual Point Count".
[25] ASTM G5; "Standard reference test method for making potentiostatic and potentiodynamic anodic polarization measurements", 2004.
[26] ASTM G3; "Standard practice for conventions applicable to electrochemical measurements in corrosion testing", 1999.
[27] ASTM A-923 "Standard Test Methods for Detecting Detrimental Intermetallic Phase in Wrought Duplex Austenitic/Ferritic Stainless Steels1.